Bernardí Bayarri*, Jaime Giménez, David Curcó and Santiago Esplugas

Absorbed radiation and kinetic model in photocatalysis by TiO_2

https://doi.org/10.1515/ijcre-2021-0045
Received February 24, 2021; accepted August 26, 2021;
published online September 10, 2021

Abstract: The current work studies a novel and affordable methodology to estimate and quantify the photon flux absorbed and the amount of light that leaves from an illuminated photocatalytic system with TiO_2 suspended in water. To achieve it, a new parameter BFS_λ^{wat} is defined and presented. It indicates, for every wavelength, the fraction of the incoming radiation which is not absorbed by the system. BFS_λ^{wat} was estimated by means of actinometric experiments in a jacketed reactor and a model based on Beer–Lambert law. For wavelengths below 388 nm and TiO_2 concentrations between 0.05 and 2 g L^{-1}, experimental values of BFS_λ^{wat} were between 0.77 and 0.27. In the second part of the work, a simple kinetic model, which breaks down the effect of incident radiation and kinetic constant, is developed. For this, the photon flux absorbed by TiO_2, previously determined, was included in the model. This new model was tested in the photocatalytic degradation of 2,4-dichlorophenol under different TiO_2 concentrations. The kinetic model fits satisfactorily the experimental values and a new kinetic constant $\boldsymbol{k'_{ap}}$ [mol·L^{-1} $Einstein^{-1}$] was obtained, which is independent of the amount of catalyst loaded to the system. This achievement may be very useful for an easy initial comparison, design or scaling up of different photocatalytic reactors with similar geometry.

Keywords: kinetic model; photocatalysis; radiation; TiO_2.

1 Introduction

Heterogeneous photocatalysis is a well-known advanced oxidation process, which has been deeply studied because of its promising potential for wastewater treatment (Al-Mamun et al. 2019; Guo et al. 2019; Herrmann 2005; Malato et al. 2009; Wetchakun et al. 2019). It is based on the absorption of radiation by a semiconductor (photocatalyst), producing e^-/h^+ pairs, which are the responsible for the generation of reactive oxygen species (ROS), highly reactive chemical molecules formed due to the electron receptivity of O_2, and, consequently, the removal of pollutants (Guo et al. 2019; Herrmann 2005; Serpone and Salinaro 1999). The most widely used photocatalyst is TiO_2 and only photons below 388 nm have enough energy to start the process when working with anatase (Guo et al. 2019; Serpone and Salinaro 1999).

Photocatalytic processes are stable, economically competitive when used with solar light and suitable for a wide variety of pollutants, but still more research is required to achieve a fully developed technology. Finding a simple, general, and versatile model that explains the process is one of the challenges that are still being investigated. The final accuracy of this hypothetical model is linked to the understanding and prediction of the radiation role in the process. It is one of the most defiant challenges in photocatalysis.

It is common to find photocatalytic studies in literature where radiation is not included in the models presented and results are just fitted to a first or zero order kinetic model. In other cases, the compounds adsorption on the catalyst is considered and the experimental results are fitted to heterogeneous catalysis models such as Hinshelwood–Hougen–Watson or similar. Unfortunately, these approximations do not take into account the effect of radiation on the process and do not achieve a full description of the system's behaviour. Although some research groups successfully include radiation as part of the kinetic models (Li Puma et al. 2004; Marugán et al. 2011; Tolosana-Moranchel et al. 2017), it is common to find works where kinetic constants are function of the amount of photocatalyst or radiation entering to the system, mainly due to the complexity of including the role of light in the process. It is well known that a "pure" kinetic constant should not be function of any of these factors. Therefore, it becomes clear that those apparent kinetic constants include the effect of variables other than the chemical reaction. These inaccuracies become problematic when it is intended to

***Corresponding author: Bernardí Bayarri**, Departament d'Enginyeria Química i Química Analítica, Facultat de Química, Universitat de Barcelona, C/ Martí i Franquès, 1, 08028, Barcelona, Spain, E-mail: bbayarri@ub.edu. https://orcid.org/0000-0003-2890-2308
Jaime Giménez, David Curcó and Santiago Esplugas, Departament d'Enginyeria Química i Química Analítica, Facultat de Química, Universitat de Barcelona, C/ Martí i Franquès, 1, 08028, Barcelona, Spain

use kinetic data in comparing systems or scaling them. Some research groups have focused part of their work in this topic. A proper way for describing the behaviour of light is solving the radiative transfer equation (RTE). It considers the scattering and absorption phenomena and allows determining the radiation distribution in the reactor. RTE can be solved analytically mainly for simple systems or by using numerical methods like the discrete ordinates method (Moreno-SanSegundo et al. 2020; Peralta Muniz Moreira and Li Puma 2021; Satuf et al. 2011), the Finite Volume Method (Roda and Santarelli 2007), or some probabilistic approaches to the mathematical solution of the RTE as the Six-Flux Absorption Scattering model (Brucato et al. 2006; Li Puma et al. 2004; Peralta Muniz Moreira and Li Puma 2021; Ramírez-Cabrera et al. 2017) or stochastic models (Acosta-Herazo et al. 2020; Tolosana-Moranchel et al. 2019).

In previous works of our group, a semiempirical way to measure the radiation absorbed by the aggregates of TiO_2 in strongly absorbent media was introduced (Bayarri et al. 2012). It was based on actinometric experiments (uranyl-oxalic method) (Sánchez Mirón et al. 2000; Volman and Seed 1964) carried out in a flat reactor. It allowed estimating P_{abs} by fitting a probabilistic model to the experimental data. P_{abs} was defined as the probability of a photon to be absorbed when it collides against a photocatalyst particle.

The aim of this article is to continue the previous work and study the behaviour of radiation in a suspension of TiO_2 in a non-attenuating medium. Accordingly, the main objective is to develop a novel semi-empirical methodology that allows estimating the radiation absorbed by a suspension of TiO_2 in a non-attenuating medium. Non-attenuating means that only the photocatalyst will absorb photons. This usual situation occurs when the suspension medium does not absorb in the UV range or when the compounds are in a concentration much lower than that of the photocatalyst (Li Puma et al. 2004). The new methodology is based on the modification of Lambert-Beer law and the estimation of the "Back-Forward-Scattered" parameter (BFS_λ^{wat}). BFS_λ^{wat} is defined as the probability that a photon of wavelength λ leaves the photo-reactor without being absorbed, after entering in the TiO_2 slurry. This parameter and the presented methodology may be useful for characterization or comparison purposes of different systems (with similar geometry) and materials.

A second objective of this work was to develop a simple kinetic model able of decoupling the effect of catalyst concentration or irradiance from the kinetic constant. Thus, a simple inclusion of radiation into the model was proposed. This kinetic model was tested in the photocatalytic degradation of 2,4-dichlorophenol (DCP).

The proposed methodology is not as rigorous as some of the cited works dealing with radiation in photocatalytic systems. However, this novel methodology is an affordable but accurate tool that allows a first characterization of heterogeneous photocatalytic systems and their comparison or even scale-up without requiring demanding mathematical models. The novel methodology is based on the well-known and widely used Beer–Lambert's law that explains the attenuation of radiation in homogeneous media. Therefore, it is conceptually simple and approachable by many researchers even if they are not experts in the behaviour of radiation in heterogeneous systems. Furthermore, the experiments necessary to characterize the system and run the model are also simple and easy to apply. The values of BFS_λ^{wat} presented in this work can even be used in other systems with a reactor of similar geometry to the one here used.

2 Experimental methods and procedures

2.1 Materials

TiO_2 was chosen as photocatalyst to carry out all the experiments. Degussa (Evonik) P25 (80% anatase, 20% rutile, specific surface area 50 $m^2 \cdot g^{-1}$, density 3.92 $g \cdot cm^{-3}$) as received from factory was used since it is the most found in literature.

Actinometric experiments were performed according to the widely known uranyl-oxalic system (Sánchez Mirón et al. 2000; Volman and Seed 1964). Water solution with 0.05 M of oxalic acid and 0.01 M of nitrate of uranyl in a free pH medium was used. All chemicals used were reagent grade and supplied by Panreac. The oxalic degradation rate was followed by means of a direct titration with permanganate.

As a model pollutant to test the kinetic model, 2,4-dichlorophenol (99%) supplied by Aldrich without further purification was used.

All suspensions and solutions were prepared using ultra-pure filtered Millipore water (18 $\mu S \cdot cm^{-1}$).

2.2 Experimental devices and procedures

All the experiments were carried out in a Solar simulator (Solarbox), from CO.FO.ME.GRA, already described

(Bayarri et al. 2005; Giménez et al. 1997). The source of radiation was a Xenon lamp (PHILIPS XOF-15-OF, 1500 W), with a continuous spectrum close to the solar one in the UV range. It was placed in the upper part of the Solarbox, in the axis of the parabolic mirrors.

Two different photo-reactors were used in this study. A tubular reactor was used to carry out the DCP degradation experiments. It was made in quartz (26 cm length and 1.95 cm inner diameter) and was located in the axis of a parabolic mirror (Rodríguez et al. 2005). Due to the geometry of the mirrors, most of the light enters perpendicularly to the axis of the reactor. The studied solution was recirculated to the reactor from a reservoir tank which temperature was controlled by means of a thermostatic bath. Different experiments were carried out and the amount of TiO_2 added to the system was changed from 0 to 2 g $TiO_2 \cdot L^{-1}$. Initial DCP concentration, $C_{0,DCP}$, was 125 mg$\cdot L^{-1}$, the same for all experiments. The suspension was circulated during 1 h without light. Then, the lamp was turned on and the photocatalytic degradation started. Samples were taken regularly and DCP and TOC concentrations were measured.

The evolution of DCP and the intermediates concentration was monitored during the degradation experiment by HPLC with a Waters Chromatograph (600 Controller Pump, 717 Photodiode Array Detector, Millenium 2.1 software, 717plus Autosampler). The detection wavelengths were 287 and 254 nm. The column was a TRACER EXTRASIL ODS2, 5 µm pore; 25 × 0.46 cm. A mixture of 40% of acetonitrile and 60% of water adjusted at pH 3 with phosphoric acid was chosen as the optimal mobile phase. TOC was monitored with a Shimadzu TOC-VCSN.

A jacketed tubular reactor was used to measure the radiation entering into the reactor and BFS_{λ}^{wat} by means of the oxalic (0.05 M) – uranyl (0.01 M) actinometer (Sánchez Mirón et al. 2000; Volman and Seed 1964).

The oxalic degradation rate follows a first order kinetics with respect to the arriving radiation and zero order with respect to the concentration of uranyl or oxalic. It is important to emphasize that uranyl-oxalic system was chosen as a model actinometer, but this methodology can be used with any other actinometer adequate for monitoring the desired radiation spectrum.

The incident photon flux F_0 can be calculated based on Lambert–Beer law and experimental oxalic degradation rate measurements (Curcó et al. 1996). The same solar simulator and procedure described in the upper paragraph were used and only the reactor was changed. This second reactor was also made in quartz, and it consisted of two concentrical tubular chambers (Figure 1). The inner reactor had the same dimensions than the tubular reactor previously presented (26 cm length and 1.95 cm inner diameter) and it was filled with ultra-pure water and different amounts of catalyst. Different experiments were made changing the TiO_2 concentration from 0 to 2 g $TiO_2 \cdot L^{-1}$ in the inner reactor. In the outer jacket or annular reactor (26 cm length and 2.95 cm outer diameter), the actinometric solution was circulated to the reservoir as described in the case of previous tubular reactor. Due to the narrow dimensions of the jacket (0.5 cm), most of the light crossed through the actinometric solution and arrived to the inner TiO_2 suspension. Then, a part of light was absorbed by the suspension and the rest was reflected or transmitted to the jacket again. Therefore, this scattered light could be also measured by the actinometrical solution. With

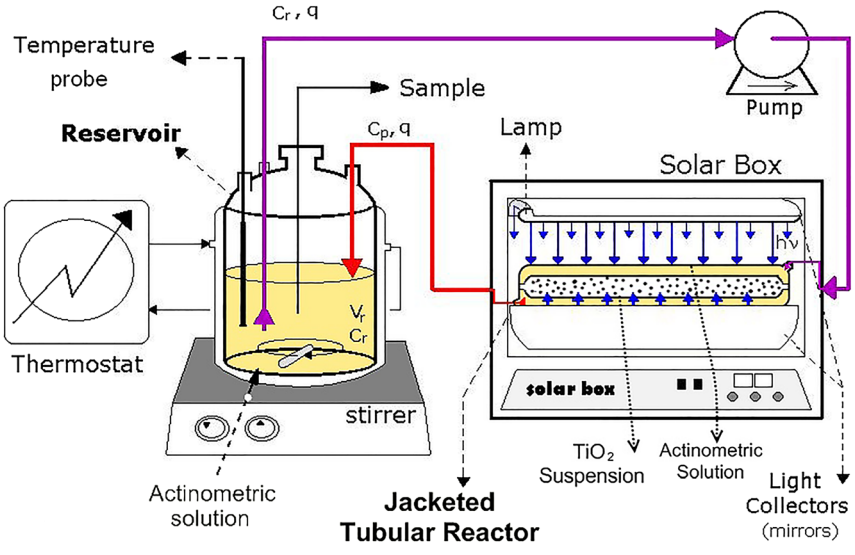

Figure 1: Experimental set up for the jacketed reactor experiments, as described in the text.

this system, it is possible to study the light absorbed by TiO_2 as function of the amount of TiO_2 loaded, the pollutant used or the pH. It was verified by means of spectrophotometric measurements that the sedimentation of TiO_2 was negligible, mainly due to the short duration of the experiment (about 10 min) and the low diameter of aggregates (250 nm).

2.3 Optical thickness

It is generally accepted that the degradation rate in a photocatalytic system is governed by the photocatalyst loading, the light source and the reactor geometry (Rizzo et al. 2014). Thus, it seems convenient to present the results of the current work as function of the optical thickness (τ). τ is an adimensional parameter which interrelates the previous commented factors and it has been broadly used in several works of this field (Moreira et al. 2010). Optical thickness can be easily calculated as:

$$\tau = \beta \cdot C_p \cdot \delta \quad (1)$$

where τ is the optical thickness β is the specific extinction coefficient ($cm^2 \cdot g^{-1}$) C_p is the catalyst concentration ($g \cdot L^{-1}$) and δ can be assimilated to the internal diameter of the inner reactor (cm). β values were obtained from (Cabrera et al. 1996; Li Puma and Brucato 2007; Moreira et al. 2010), where this parameter was determined for a suspension very similar to the one used in the current work. τ and β are specific for each wavelength. Thus, in the case of polychromatic radiation β may be averaged over the useful spectrum of the incident radiation as explained by (Li Puma and Brucato 2007). In this work and regarding optical thickness, only radiation below 388 nm was considered since it is the useful radiation for this photocatalyst. Results obtained are presented respect to both, the catalyst concentration (C_p) and optical thickness (τ). On this way, comparison with both factors can be done.

3 Results and discussion

3.1 Estimation of BFS_λ^{wat} in the jacketed tubular reactor

In the first part of experiments, the inner chamber of the jacketed tubular reactor was filled with a suspension of TiO_2 in water. This was repeated for different concentrations of TiO_2. In the annular chamber, an actinometric solution was recirculated and oxalic acid concentration was monitored. It allowed calculate the incident light. For this reactor, incident light refers to the radiation arriving

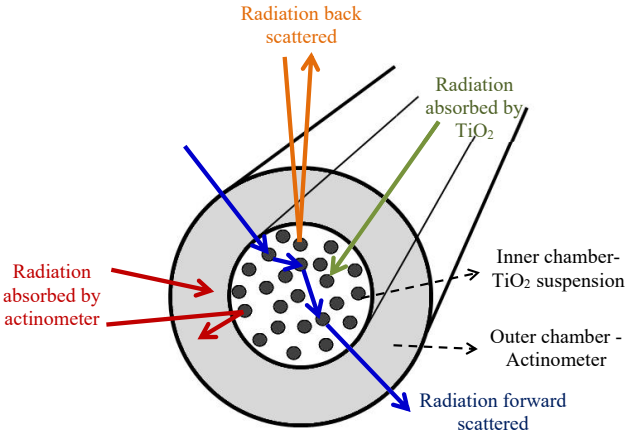

Figure 2: Schematic representation of the different ways that light can take inside of the jacketed reactor (solid arrows).

directly from the lamp (which is constant for all the experiments) or also to that light leaving from the inner reactor due to back or forward scattering (which is function of the TiO_2 concentration). To make it clearer, Figure 2 schematically describes the possible radiation distribution inside the reactor. The considered light pathways can be summarized as follows: when light arrived from the lamp to the photoreactor, firstly it entered and went through the outer, narrow jacket. A small part of radiation was absorbed, degrading a fraction of the oxalic acid. The rest of radiation arrived at the inner tubular reactor, which contained the TiO_2 suspension. Part of this incoming radiation was immediately back scattered by the TiO_2 particles, so it crosses again the outer chamber in the opposite direction and escapes from the system. The rest of light went inside the inner tubular reactor. Part of it was absorbed by the TiO_2 aggregates and the rest was finally forward scattered and left the inner tubular reactor, so it passed through the annular chamber again. Thus, again a fraction of it was absorbed by uranyl and a new fraction of oxalic acid was degraded.

The steps explained before and how they affect to the oxalic degradation rate occurring in the jacket chamber can be modelled according to the following expression:

$$R_{ox} = \overbrace{F_0 \sum f_\lambda \cdot [1 - \exp(-\alpha_\lambda \cdot d_{ext})] \cdot \varphi_\lambda \cdot T_\lambda}^{A} + \underbrace{F_0 \cdot \sum f_\lambda \cdot T_\lambda \cdot \exp(-\alpha_\lambda \cdot d_{ext}) \cdot T_\lambda \cdot BFS_\lambda^{wat}}_{C} \cdot \underbrace{[1 - \exp(-\alpha_\lambda \cdot d_{ext})] \cdot \varphi_\lambda \cdot T_\lambda}_{B} \quad (2)$$

R_{ox} is the oxalic degradation rate [$mol \cdot s^{-1}$] due to uranyl light absorption, λ the wavelength [nm], F_0 the photon flux arriving to the reactor (before entering) [$Einstein \cdot s^{-1}$], f_λ the fraction of radiation of wavelength λ according to the lamp spectrum [dimensionless], φ_λ is the quantum yield for

the actinometric system [mol·Einstein^{-1}], α_λ the uranyl attenuation coefficient at λ [m^{-1}] and 0.01 M.

T_λ is the transmittance at λ [dimensionless] and in this work refers to the transmittance of quartz reactor walls (all walls present the same thickness, and it is considered T_λ = 90% for the studied spectral range).

d_{ext} is the distance "travelled" by a photon [m]. In this case is the distance travelled by the light in the jacket to arrive to the inner reactor. If most of radiation enters perpendicularly to the reactor, it is considered that d_{ext} = 0.5 cm.

Finally, BFS_λ^{wat} is the probability that a photon, after entering the TiO_2-water suspension, leaves it without being absorbed. This novel parameter includes all radiation directly backscattered or the radiation that, after entering the inner reactor and travelling through it, finally leaves the inner reactor without being absorbed (it may be called "forward-scattered" radiation). BFS_λ^{wat}, as most of the optical parameters, depends on the wavelength.

Equation (2) is based in the broadly accepted Beer–Lambert's Law for light absorption in homogeneous systems (Curcó et al. 1996). Most of parameters in this equation (f_λ, φ_λ, T_λ, α_λ, d_{ext}) are known or tabulated in literature (Sánchez Mirón et al. 2000; Volman and Seed 1964) or found in previous papers of the group (Bayarri et al. 2005). This data can be found in Supplementary Table S1. R_{ox} was determined experimentally. The only unknown values were F_0 and BFS_λ^{wat} which could be calculated as explained below. It is also noteworthy to remark uranyl-oxalic system was chosen just an actinometer model. It should be possible to apply this approach with any other actinometer which absorbs in the spectrum range of interest, as for example *o*-nitrobenzaldehyde actinometry (De La Cruz et al. 2013; Galbavy et al. 2010).

To facilitate the understanding of the model, Eq. (2) may be split in meaningful parts:

- $F_0 \cdot f_\lambda \cdot [1 - \exp(-\alpha_\lambda \cdot d_{ext})] \cdot \varphi_\lambda \cdot T_\lambda$ calculates the oxalic degradation rate due to radiation (wavelength λ) crossing the jacket for homogeneous systems, according to Beer–Lambert's law. When appearing in the first summand ("A" term in Eq. (2)), it calculates the oxalic degradation rate due to light arriving to the actinometric solution directly from the lamp. When appearing in the second summand ("B term in Eq. (2)), it considers the degradation of oxalic due to radiation leaving from the inner reactor and, therefore, not absorbed by the TiO_2.
- $F_0 \cdot f_\lambda \cdot T_\lambda \cdot \exp(-\alpha_\lambda \cdot d_{ext}) \cdot T_\lambda$("C" term in Eq. (2)) calculates the amount of radiation arriving at the inner reactor, for a wavelength λ, after passing through the jacket. Therefore, this term considers the radiation absorbed in the outer jacket. Multiplying this term per BFS_λ^{wat}, the radiation leaving the inner reactor is estimated. T_λ appears twice because radiation must cross the wall of the inner reactor twice: one when entering in the inner reactor and one when leaving it. This term was used in the model to estimate the radiation arriving to the jacket backscattered from the inner reactor. Multiplied by term B, it allowed calculating the oxalic degradation rate due to the radiation leaving from the inner reactor.

In summary, this model considers that the oxalic acid degradation rate is the sum of the degradation due to the light that comes directly from the lamp and crosses the jacket (term A) plus the light that, after reaching to the internal reactor is scattered, escapes from the TiO_2 suspension and cross the actinometric jacket again (term B per term C).

To test the system and finding F_0, it was required to work on the boundaries. Accordingly, two limit situations were considered. The first referred to the scenario in which all the incident light was absorbed in the internal reactor. The second, opposite scenario, occurred when no light at all was absorbed in the internal reactor.

In this study, we call "black" solution to that solution which absorbs all the incoming radiation. Then, if the inner reactor was filled with a "black" solution, BFS_λ^{wat} should be equal to 0 (no light was leaving from the inner reactor). A saturated solution of $KMnO_4$ was used as "black" solution to experimentally check this scenario. In that case, Eq. (2) reduces to:

$$R_{ox} = F_0 \sum f_\lambda \cdot [1 - \exp(-\alpha_\lambda \cdot d_{ext})] \cdot \varphi_\lambda \cdot T_\lambda \qquad (3)$$

which is the common model applied for finding F_0 in a simple actinometric experiment. The other limit would correspond to the situation in which the internal reactor did not absorb any radiation, so BFS_λ^{wat} would be equal to 1 (all the light was leaving from the inner reactor). Experimentally, this scenario was created by filling the inner reactor with ultra-pure water.

Based on everything explained above, a series of experiments were done in the jacketed tubular reactor to determine the value of BFS_λ^{wat}. Firstly, two set of experiments were done to determine the radiation arriving at the reactor (F_0) and to check the validity of the proposed method. A first experiment was done filling the inner reactor with a saturated solution of $KMnO_4$. This type of solution worked as a black body and absorbs all the arriving radiation in the studied range. As commented, for these conditions BFS_λ^{wat} was assumed to be equal to 0.

A second experiment was done filling the inner reactor with ultra-pure water, which is only absorbing infrared radiation, not considered in this study. Thus, BFS_{λ}^{wat} was assumed to be equal to 1.

Since BFS was assumed, all the parameters of Eq. (2) were previously known or tabulated, except R_{ox}, which was measured experimentally, and F_0. Thus, once R_{ox} was measured, F_0 could be directly calculated by means of Eq. (2).

To measure R_{ox}, the experiment was started by recirculating the actinometrical solution through the reactor jacket. For $t = 0$, the lamp was turned on and the photoreactor was illuminated, initiating the actinometrical reaction. To determine the reaction rate, samples were withdrawn at regular intervals. With these data, R_{ox} was calculated according to Eq. (4):

$$V_T \cdot \frac{dC_{ox}}{dt} = -R_{ox} \quad (4)$$

where V_T is the total volume of the system, t refers to time, C_{ox} is the oxalic concentration experimentally measured and R_{ox} is the oxalic acid degradation rate. Since oxalic degradation follows a zero-order kinetics degradation rate, experimental oxalic concentration values versus time were fitted to a straight line using the least squares method. Figure 3 presents some of the experimental data found. Data presented are the average values for the duplicated experiments. R_{ox} was calculated from the slope obtained in the fitting. Table 1 summarizes the average experimental results for all the TiO_2 used concentrations. For all tested conditions, the fitting was very good. R_{ox} was calculated for wavelengths up to 546 nm, according to the data found in literature. It must be remarked that for wavelengths higher than 400 nm the radiation absorbed by uranyl is very small.

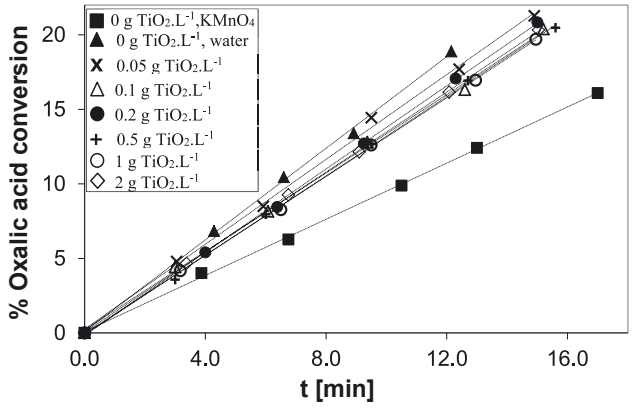

Figure 3: Variation of oxalic degradation versus time in actinometric experiments in the jacketed tubular reactor for different amounts of TiO_2 loaded in the inner reactor. "0 g $TiO_2 \cdot L^{-1}$, $KMnO_4$" corresponds to the experiment with the inner reactor filled with $KMnO_4$ solution and "0 g $TiO_2 \cdot L^{-1}$, water" corresponds to the experiment with the inner reactor filled only with water. $[oxalic]_0 = 0.05$ M, $[uranyl]_0 = 0.01$ M.

Table 1: Results for actinometric experiments with the jacketed reactor. Initial oxalic concentration ($C_{0,OA}$) and the measured R_{ox} are shown, as well as the slope found in the lineal regression and R^2. [uranyl] = 0.01 M. Experiments were run until about a 20% of oxalic was degraded and less than 10% of oxalic was withdrawn.

C_p [g $TiO_2 \cdot L^{-1}$]	$C_{0,OA}$ [M]	τ [–]	Lineal regression slope [min^{-1}]	$R_{ox} \times 10^5$ [mol s^{-1}]	R^2
0 ($KMnO_4$)	0.049	–	1.06	0.87	0.9986
0 (water)	0.049	0	1.50	1.23	0.9986
0.05	0.050	5.23	1.42	1.19	0.9980
0.10	0.050	10.5	1.41	1.17	0.9985
0.20	0.046	20.9	1.46	1.13	0.9977
0.50	0.051	52.3	1.33	1.12	0.9994
1.00	0.051	105	1.32	1.12	0.9997
2.00	0.050	209	1.34	1.12	0.9998

Once R_{ox} was measured, F_0 for wavelengths up to 546 nm was directly calculated (from Eq. (2)) finding a value equal to 188.6 μ Einstein s^{-1}, for the experiment with $KMnO_4$, and 190.0 μ Einstein s^{-1}, for the experiment with water (without TiO_2 in both cases). As it was indicated previously, F_0 represents the radiation arriving to the outer jacket. Thus, it should be the same for both experiments and, effectively, the experimental values obtained (188.6 and 190.0) are practically the same.

The results were promising. Despite working in the two possible extremes ($BFS_{\lambda}^{wat} = 1$ and $BFS_{\lambda}^{wat} = 0$), the value of F_0 found was practically the same in both cases, as just commented.

Once the incident photon flux was determined, a second set of experiments was carried out filling the inner reactor with different amounts of TiO_2 in water (i.e., different optical thicknesses) and measuring the resulting R_{ox}. In these experiments, part of the incident light was absorbed by the TiO_2 and the rest returned to the jacket, so the oxalic degradation rate changed accordingly. The experimental results are shown in Figure 3 and Table 1. As it can be seen, R_{ox} decreased when increasing TiO_2 concentration, remaining practically constant for concentrations higher than 0.5 g TiO_2 L^{-1} or $\tau = 52.3$.

In this second series of experiments, the value of F_0 was already known since it had been previously determined. Therefore, from Eq. (2) and with the experimental values of R_{ox} measured, it should be possible to calculate the value of BFS_{λ}^{wat}. However, in this occasion Eq. (2) could not be solved directly, since BFS_{λ}^{wat} was different for every

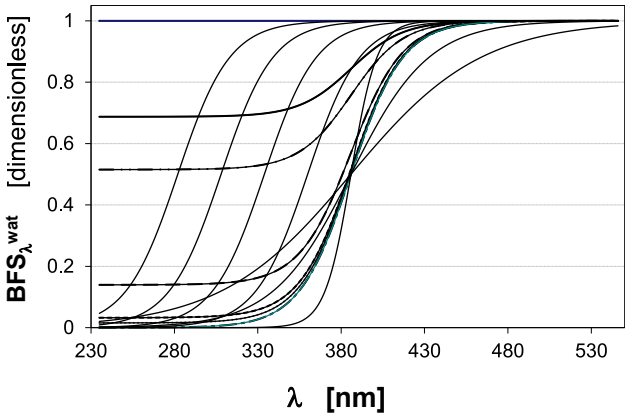

Figure 4: Set of different possible solutions for Eq. (5), depending on the value give to the parameters. It presents a similar shape to the reflection measures (or related extinction coefficient) found in literature for TiO_2.

wavelength and the solution must include this fact. To overcome this problem and according to its definition, it was assumed that BFS_λ^{wat} followed a similar trend to that of the experimental reflectance of TiO_2 suspended in water. Therefore, BFS_λ^{wat} was fitted to a sigmoidal function (Richard's equation) since it presents several solutions but with trends always similar to the experimental determination of TiO_2 reflectance in water (Augugliaro et al. 1991; Serpone et al. 2000; Wang et al. 2002). Hence, BFS_λ^{wat} for each λ was found by calculating it by means of Richard's equation (Eq. (5)):

$$BFS_\lambda^{wat} = 1 - \frac{a}{(1+\exp(b - c\cdot\lambda))^{\frac{1}{d}}} \quad (5)$$

where λ is the wavelength considered and BFS_λ^{wat} the probability that a photon of wavelength λ is not absorbed in the TiO_2 suspension. *a, b, c* and *d* are empirical parameters that must be iterated to find the right solution. In Figure 4, different theoretical solutions to Richard's equation are presented, showing the flexibility and typology of solutions covered by this function.

To solve Eq. (2) and estimate BFS_λ^{wat} according to the experimental results, the next procedure was followed:

(1) Firstly, first summand of Eq. (2) was calculated since all values were known. Obviously, it was constant for all TiO_2 concentrations since it is the degradation due to the light arriving directly from the lamp. For the photocatalytic range of interest (λ < 388 nm):

$$\sum_{\lambda<388\text{nm}} f_\lambda \cdot [1-\exp(-\alpha_\lambda \cdot d_{ext})] \cdot \varphi_\lambda \cdot T_\lambda = 0.463\,\text{mol·Einstein}^{-1}$$

(2) F_0 was previously determined. Thus, all values in second summand of Eq. (2) were known, except BFS_λ^{wat}. Thus, a first set of values *a, b, c* and *d* for Eq. (5) were chosen and a theoretical R_{ox} was calculated. It was compared to the experimental value and if both did not coincide, a second set of values for Richard's equation were used. This iteration was repeated until the theoretical R_{ox} was equal to the experimental one. As a constriction, BFS_λ^{wat} was forced to be between 0 and 1 and the slope of the curve between 300 and 450 nm. This spectrum range was chosen because it is quite coincident with experimental reflectance measurements and allows the convergence of the iteration. Despite the wide range used, it must be highlighted that the fraction of light over 400 nm corresponds to the tale of the curve and is quite insignificant, as it will be showed later.

(3) By means of a computer program, this iteration was run for all the TiO_2 concentrations tested. For each TiO_2 concentration, a different curve for BFS_λ^{wat} was found. Each curve was used as initial solution for the next concentration.

In Figure 5 the solutions to the model found for each optical thickness used are shown. The corresponding values of *a*, *b*, *c* and *d* are presented in Table 2. All the curves showed a similar shape. When the amount of TiO_2 loaded decreases, the amount of light leaving from the inner chamber of the reactor increased. This phenomenon could be observed up to C_p = 0.5 g $TiO_2 \cdot L^{-1}$ (τ = 52.3). For higher amounts of photocatalyst, the differences between BFS_λ^{wat} curves were negligible, and the behaviour was practically the same.

As a limitation to the reported data, BFS_λ^{wat} values are expected be valid for other photocatalytic reactors if they

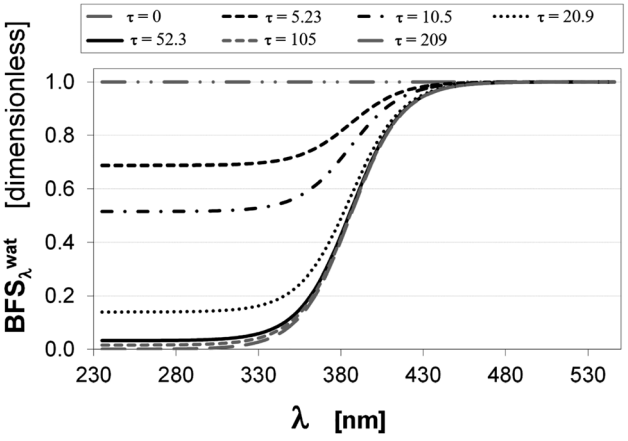

Figure 5: BFS_λ^{wat} versus wavelength, for the different TiO_2 concentration tested expressed as optical thickness (τ). BFS_λ^{wat}s were estimated iterating Eq. (5), together to Eq. (2), to match up the oxalic degradation rate experimentally found.

Table 2: Radiation lost due to back and forward scattering in inner chamber of the jacketed reactor filled with a suspension of TiO_2 in water ($\overline{BFS^{wat}_{\lambda<xxx}}$). The values are given for different concentrations of TiO_2 or τ. Parameters used to calculate $\overline{BFS^{wat}_{\lambda<xxx}}$ with Eq. (5) are also listed.

TiO_2-water suspension							
C_p [g $TiO_2 \cdot L^{-1}$]	τ [–]	$BFS^{wat}_{\lambda<388}$ [–]	$BFS^{wat}_{\lambda<546}$ [–]	a [–]	b [–]	c [–]	d [–]
0.00	0.00	1.00	1.00	0	−149	−0.385	6.0
0.05	5.23	0.77	0.98	0.313	−149	−0.385	6.0
0.10	10.5	0.65	0.96	0.485	−149	−0.385	6.0
0.20	20.9	0.37	0.94	0.860	−149	−0.385	6.0
0.50	52.3	0.30	0.93	0.968	−149	−0.385	6.0
1.00	105	0.28	0.93	0.985	−149	−0.385	6.0
2.00	209	0.27	0.93	1.000	−149	−0.385	6.0

present same cylindrical shape and inner diameter. If geometry is different, the light leaving from the reactor can change in an important way. For example, for same conditions but bigger diameter the value of BFS^{wat}_{λ} would be lower. Thus, in this case it would be necessary to determine the new BFS^{wat}_{λ} values. However, the methodology can be perfectly useful.

Figure 5 shows that BFS^{wat}_{λ} was different for each TiO_2 concentration and wavelength. To allow an easier comparison between experiments and to present a "global reflectance" of each suspension, $\overline{BFS^{wat}_{\lambda=p\to m}}$, was estimated. This is a weighted average value of BFS^{wat}_{λ}. To be accurate and facilitate future comparisons with other devices, it was normalized by considering the incoming spectrum, according to the next equation:

$$\overline{BFS^{wat}_{\lambda=p\to m}} = \frac{\sum_{\lambda=p}^{\lambda=m} f_\lambda \cdot T_\lambda \cdot \exp(-\alpha_\lambda \cdot d_{ext}) \cdot T_\lambda \cdot BFS^{wat}_{\lambda}}{\sum_{\lambda=p}^{\lambda=m} f_\lambda \cdot T_\lambda \cdot \exp(-\alpha_\lambda \cdot d_{ext}) \cdot T_\lambda} \quad (6)$$

This equation calculates the weighted average value of light not absorbed by TiO_2 from wavelengths "p" to "m", according to the number of photons presents for each wavelength, i.e., to the photonic spectrum. Actually, it was proceeded in a similar way to the calculation of the average β estimated for the calculation of the optical thickness by Eq. (1). In Table 2, the average values of this parameter for the whole spectrum considered (up to 546 nm) and for the useful zone for TiO_2 (up to 388 nm) were listed. If the spectrum zone with wavelengths up to 546 nm is analyzed, it can be seen how the amount of radiation leaving from the TiO_2 suspension is very important, with losses among 93 and 98%. It was expected since up to 86% of incident radiation was photons over 400 nm and, as known, radiation over 400 nm is not absorbed by TiO_2. Thus, these high radiation losses seemed justified. However, if only spectrum below 388 nm is considered, the results were quite different: radiation losses were important for low amounts of TiO_2, but they decrease quickly when TiO_2 concentration increases. For 2 g $TiO_2 \cdot L^{-1}$ (τ = 209) only about 27% of incoming UV radiation to the inner reactor was lost.

Once BFS^{wat}_{λ} was estimated, it was easy to calculate the radiation up to 388 nm absorbed by TiO_2 (value required at the second part of the work). As it was proved in previous works (Bayarri et al. 2007), it can be assumed that only the TiO_2 absorbed radiation in the suspension since water or even DCP solution do not significantly absorb radiation. According to this assumption, all missing radiation was absorbed by TiO_2 so $(1 - BFS^{wat}_{\lambda})$ was the fraction of radiation absorbed by the TiO_2 suspension. Thus, multiplying $(1 - BFS^{wat}_{\lambda})$ per the photon flux entering the inner reactor, $F^{abs\,TiO_2}_{\lambda<388}$ could be directly calculated by Eq. (7):

$$F^{abs\,TiO_2}_{\lambda<388} = F_0 \cdot \sum_{\lambda<388} f_\lambda \cdot T_\lambda \cdot \exp(-\alpha_\lambda \cdot d_{ext}) \cdot T_\lambda \cdot (1 - BFS^{wat}_{\lambda}) \quad (7)$$

being $F^{abs\,TiO_2}_{\lambda<388}$ the radiation below 388 nm absorbed by TiO_2 particles. According to its definition, Eq. (7) can be used with any non-absorbing solution.

Figure 6 shows the photon flux absorbed by TiO_2 in pure water. The curve presents a typical trend for photocatalytic systems. For low TiO_2 concentrations, the photon flux absorbed by the photocatalyst increases quickly with the amount of TiO_2 loaded to the system. Then, for a

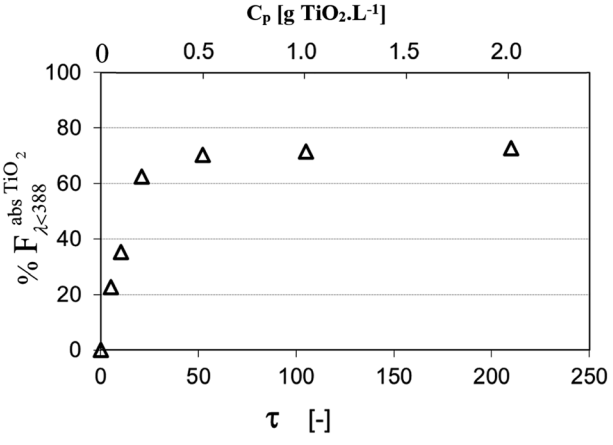

Figure 6: Percentage of photon flux absorbed by TiO_2 suspended in a water solution for different amount of TiO_2 loaded, expressed versus TiO_2 concentration and optical thickness. Only radiation below 388 nm was considered. F_0 = 8.24 μEinstein·s^{-1} (UV range).

threshold value, the system is saturated and TiO_2 cannot absorb more radiation. Thus, the photon flux absorbed by the TiO_2 remains constant and independent of the amount of TiO_2 present in the system. In the current system, the threshold value stands around 0.2 and 0.5 g $TiO_2 \cdot L^{-1}$ which is equal to optical thickness between 20.9 and 52.3.

3.2 Tubular reactor: DCP degradation experiments and model fitting

A second target of the study was to develop a kinetic model that describes pollutant degradation by TiO_2 and considers the values of radiation absorption determined previously. In this case the DCP degradation was studied, as a model case. A DCP mass balance lead to the following equation:

$$-V_T \cdot \frac{dc_{DCP}}{dt} = r_{DCP} \cdot V_p \quad (8)$$

V_T is the total volume of the system, V_p is the volume of the photoreactor, C_{DCP} is the pollutant concentration in the reservoir, and τ is the time. This expression assumes that reaction only occurs in the photoreactor, which represents a small part of the total volume (approximately 1/10 of the volume).

In wastewater treatment, it is common to find pollutants of high molecular weight. In these cases, intermediate compounds are always generated during degradation before achieving the mineralization of the contaminant. Thus, a proper kinetic model should consider the competence between the initial pollutant and the intermediates produced for the ROS generated. It is very complex to determine accurately the whole degradation path or follow all the intermediates. Therefore, total organic carbon (TOC) is used in this work to include the intermediates. TOC refers to all the organic compounds in the solution not mineralized: initial pollutant and its generated intermediates. Aligned to the previous discussion, the following semi-empirical kinetic expression is proposed to include the competence among DCP and its intermediates:

$$r_{C,DCP} = k_{ap} \cdot \frac{C_{C,DCP}}{C_{TOC}} = k_{ap} \cdot \frac{C_{C,DCP}}{C_{C,DCP} + C_{C,I}} \quad (9)$$

$r_{C,DCP}$ is DCP degradation rate based on carbon moles [$mol \cdot s^{-1} \cdot L^{-1}$], $C_{C,DCP}$ is DCP concentration based on carbon moles, C_{TOC} is TOC concentration, $C_{C,I}$ is intermediates concentration based on carbon moles (all concentrations in $mol \cdot L^{-1}$), and k_{ap} is an apparent kinetic constant. Since the same lamp and reactor geometry were used in all experiments, also $F_{abs}^{TiO_2}$ was considered constant throughout the experiment. k_{ap} includes the chemical kinetic constant for DCP degradation and other steps of the process. In addition, k_{ap} also includes the photonic flux absorption by TiO_2 or other kinetic parameters as the kinetic constants for the electron/hole recombination or the concentration of electron/holes, which can be considered constant for the current conditions of the experiments. It may be summarized in Eq. (10):

$$k_{ap} = k'_{ap} \cdot F_{abs}^{TiO_2} \quad (10)$$

where k'_{ap} includes all the other steps and constant parameters not considered.

According to Eqs. (9) and (10), DCP degradation rate is a function of the photon flux absorbed by the photocatalyst and the ratio between DCP and TOC of the solution. It is assumed that both, the molecules of DCP and the intermediates, present the same affinity for the active sites of the catalyst and ROS species, as •OH radicals. Thus, when the number of intermediates increases in the media, less molecules of DCP will be degraded. At the beginning of the experiment, C_{DCP}/C_{TOC} ratio will be close to one and degradation rate will be fast. When the reaction goes on, C_{DCP} will decrease, and more intermediates will be generated. Thus, C_{TOC} will not decrease as fast as C_{DCP} and C_{DCP}/C_{TOC} ratio will become smaller with time, decreasing also C_{DCP} degradation rate. It is an indirect way to include in the model the competence between DCP and intermediates for available reactive species. According to this semi-empirical equation, DCP degradation rate will follow a pseudo-zero order kinetics respect to DCP degradation concentration.

A similar model was already checked in previous works, exhibiting a better fitting than a conventional first order model and being much more independent of the system variables (Augugliaro et al. 1991).

Finally, to solve differential Eq. (9), it is necessary to know TOC concentration at each point. Experimental results were analysed, and it was found that the most accurate fitting was considering TOC degradation as a homogeneous zero order kinetics, according to Eq. (11):

$$r_{TOC} = k_{TOC} \quad (11)$$

Kinetic model (Eqs. (9) and (11)) was fitted to experimental data for each TiO_2 concentration tested. As an example, DCP and TOC measurements are depicted in Figure 7 for some of the TiO_2 concentrations tested. To facilitate the use of Eq. (9) and the comparison of both series, DCP and TOC concentrations are presented only in base to the carbon present in the compound. So, when $t = 0$,

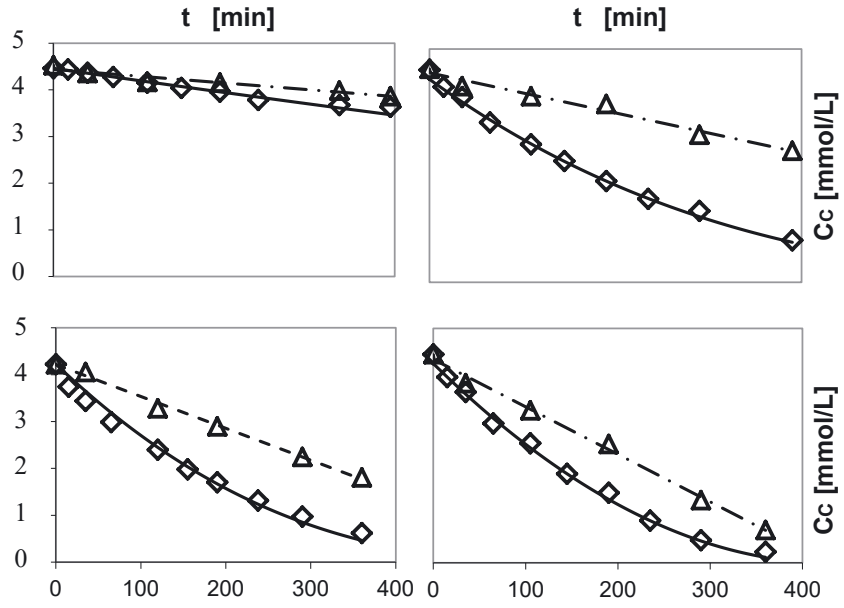

Figure 7: DCP degradation versus time for 0.01 (a), 0.2 (b), 0.5 (c) and 2 (d) g TiO_2 L^{-1}. Both DCP (◇) and TOC (Δ) are included. Concentrations are only based on carbon concentration (C_C), so both series are comparable. Flow rate = 27.5 mL s^{-1}, free pH (initially pH = 5.5), T = 23 °C. Lines represent the kinetic model used (Eqs. (8) and (10)).

Table 3: Kinetic constants according to Eqs. (10) and (8) for DCP degradation experiments.

C_p [g $TiO_2 \cdot L^{-1}$]	τ [–]	k_{ap} [mol·L^{-1}·s^{-1}]	k_{TOC} [mol·L^{-1}·s^{-1}]
0.01	1.05	2.9	1.6
0.05	5.23	6.2	2.2
0.10	10.5	10.1	4.1
0.20	20.9	18.0	4.8
0.50	52.3	19.2	7.5
1.00	105	18.5	9.6
2.00	209	18.9	11.3

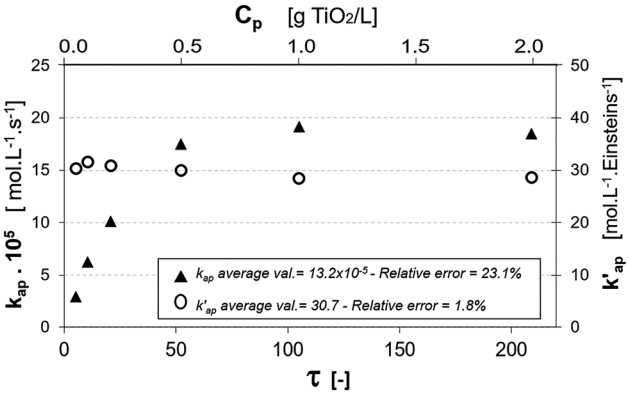

Figure 8: Kinetic constants estimated versus TiO_2 concentration (c_p) or optical thickness (τ). k_{ap} is an apparent kinetic constant and includes the effect of radiation (Eq. (9)). k'_{ap} is a similar constant but the photon flux absorbed by TiO_2 was taken into account (Eq. (10)). Relative error calculated only for $C_p \leq 0.5$ g $TiO_2 \cdot L^{-1}$ (range in which k_{ap} changes with the TiO_2 concentration).

C_{TOC} will be equal to $C_{C,DCP}$. Experimental results followed the same trend than those found in previous works for similar conditions (Abellán et al. 2007). Differential equations were solved by using Heun's method (Grasselli, 2008). k_{ap} and k_{TOC} were estimated by means of Least Mean Squares. Both equations fitted notably well to the experimental data (see Figure 7). In Table 3, kinetic constants are reported for all the experiments.

To show the results in a more visual way, Figure 8 presents the values of the estimated kinetic constants k_{ap}. The curve obtained is a typical response in the behaviour of photocatalytic systems. k_{ap} is totally dependent on the amount of TiO_2 loaded. Up to c_p = 0.5 g $TiO_2 \cdot L^{-1}$ (τ = 52.3) the kinetic constants increase quickly with the TiO_2 concentration. Then, the system gets saturated and kinetic constants are steady. On the other hand, and as expected, k'_{ap} is practically constant. It will be further explained in the next section.

3.3 Photon flux inclusion in kinetic model

As mentioned above, a kinetic constant should not be a function of the catalyst concentration or irradiance that the system receives. Actually, previous works have presented rigorous kinetic models without a direct dependence on catalyst loaded (Marugán et al. 2011; Tolosana-Moranchel et al. 2017). On the other hand, when comparing Figures 6 and 8, a parallelism is observed in the shape of the k_{ap} and $F_{abs}^{TiO_2}$ curves. Therefore, a certain relationship between both values can be guessed.

This parallelism seems to be aligned with the discussion raised when introducing Eq. (10). Thus, using Eq. (10) and the values of k_{ap} (Table 3) and $F_{abs}^{TiO_2}$ (Figure 6) previously found, the new constant k'_{ap} was calculated. As observed in Figure 8 and as expected, k'_{ap} is independent of the absorbed radiations. Although $F_{abs}^{TiO_2}$ was calculated for a suspension of TiO_2 in water instead of a DCP solution, authors assume that the error is negligible because DCP absorbs UV radiation very weakly, as it was proved in previous works (Bayarri et al. 2007).

Figure 8 presents and compares the values of k'_{ap} and k_{ap}. It can be checked how k'_{ap} values are practically constant, as expected, in contrast with k_{ap}. To carry out a preliminary analysis of the different kinetic constants estimated, average values for k_{ap} and k'_{ap} and their relative errors were also included in Figure 8. It only shows the relative error for the concentrations up to 0.5 g TiO_2 L^{-1} (the only constants that are function of the TiO_2 loaded). While k_{ap} presents a relative error around 25%, error for k'_{ap} is almost negligible, below 2%. Hence, the experimental results seem to confirm how, when introducing the absorbed radiation in the kinetic model according to the proposed methodology, the kinetic constants obtained are independent of the TiO_2 concentration.

Based on the satisfactory results, the usefulness of the proposed method for determining the radiation absorbed by TiO_2 in other non-absorbing mediums seems to be encouraging. It is also clear the importance of including radiation in the kinetic models, to obtain kinetic constants not depending on incoming light. In fact, it is a key factor to success in having valid kinetic models suitable for design, scaling up or comparison of reactors.

4 Conclusions

The main highlights of the current work are the listed below:

- BFS_{λ}^{wat}, a new optical parameter, was presented and estimated. It indicates, for each wavelength, the fraction of the incoming radiation not absorbed by the system. This parameter, together with a novel method based on actinometrical experiments, allows measuring the radiation absorbed by TiO_2 in a non-absorbing medium.
- DCP photocatalytic degradation was studied. Radiation was included in the kinetic model by means of the photon flux absorbed by TiO_2 in a non-absorbing medium. It allowed estimating new kinetic constants independent of the amount of photocatalyst loaded to the system. These constants should be much more useful for design and comparison purposes.

Nomenclature

BFS_{λ}^{wat}	fraction of light of wavelength λ not absorbed by TiO_2 which escapes from the system
$\overline{BFS_{\lambda=p\to m}^{wat}}$	average fraction of light not absorbed by TiO_2 which escapes from the system, with wavelength between p and m
C_{DCP}	DCP concentration, mol·L^{-1}
$C_{C,DCP}$	DCP concentration based on carbon concentration, mol·L^{-1}
C_{TOC}	TOC concentration, mol·L^{-1}
$C_{C,I}$	Intermediates concentration based on carbon concentration, mol·L^{-1}
$C_{0,C,DCP}$	Initial DCP concentration based on carbon concentration, mol·L^{-1}
$C_{0,OA}$	Initial oxalic acid concentration mol·L^{-1}
C_P	TiO_2 concentration, g·L^{-1}
d_p	Aggregate/particle diameter
d_{ext}	Distance covered by a photon through uranyl solution, m
DCP	2,4 Dichlorophenol
h	Distance between to TiO_2 particles in a suspension, m
F_0	Photon flux arriving to the photoreactor just before entering it, Einstein s^{-1}
F_0'	Photon flux entering the photoreactor, Einstein s^{-1}
f_{λ}	Fraction of spectrum for wavelength λ nm, dimensionless
$F_{abs}^{TiO_2}$	Radiation absorbed by TiO_2, Einstein s^{-1}
$F_{\lambda<388}^{abs\,TiO_2}$	Radiation below 388 nm absorbed by TiO_2, Einstein s^{-1} for a wavelength from p to m.
k'_{ap}	Apparent kinetic constant without including radiation absorbed by TiO_2, mol·L^{-1} s^{-1}
k_{ap}	Apparent kinetic constant including radiation absorbed by TiO_2, mol·L^{-1} s^{-1}
P_{abs}	Photon absorption probability, dimensionless
R_{ox}	Oxalic degradation rate, mol s^{-1}
$r_{C,DCP}$	DCP degradation rate based on carbon concentration, mol·L^{-1} s^{-1}
r_{DCP}	DCP degradation rate based on carbon concentration, mol·L^{-1} s^{-1}
T	Transmittance, dimensionless
TOC	Total Organic Carbon mg L^{-1}
V_T	Total volume of the system, L
V_p	Photoreactor volume, L
λ	Wavelength, nm
φ	Quantum yield, mol $Einstein^{-1}$
α	Uranyl attenuation coefficient (in this work, for 0.01 M)
δ	Internal reactor diameter
τ	Optical thickness
β	Specific extinction coefficient, cm^2 g^{-1}
ρ_{TIO2}	TiO_2 density, g cm^{-3}

Subscripts and Superscripts

abs	Absorption
ur	Uranyl

λ	Wavelength
TiO_2	TiO_2

Author contributions: All the authors have accepted responsibility for the entire content of this submitted manuscript and approved submission.

Research funding: The authors wish to thank the Spanish Ministry of Economy and Competitiveness (Project CTQ2017-86466-R, MINECO/FEDER, UE) and AGAUR-Generalitat de Catalunya (Project 2017SGR-131).

Conflict of interest statement: The authors declare no conflicts of interest regarding this article.

References

Abellán, M. N., B. Bayarri, J. Giménez, and J. Costa. 2007. "Photocatalytic Degradation of Sulfamethoxazole in Aqueous Suspension of TiO2." *Applied Catalysis B: Environmental* 74: 233–241.

Acosta-Herazo, R., P. J. Valadés-Pelayo, M. A. Mueses, M. H. Pinzón-Cárdenas, C. Arancibia-Bulnes, and F. Machuca-Martínez. 2020. "An Optical and Energy Absorption Analysis of the Solar Compound Parabolic Collector Photoreactor (CPCP): The Impact of the Radiation Distribution on its Optimization." *Chemical Engineering Journal* 395, https://doi.org/10.1016/j.cej.2020.125065.

Al-Mamun, M. R., S. Kader, M. S. Islam, and M. Z. H. Khan. 2019. "Photocatalytic Activity Improvement and Application of UV-TiO2 Photocatalysis in Textile Wastewater Treatment: A Review." *Journal of Environmental and Chemical Engineering*, https://doi.org/10.1016/j.jece.2019.103248.

Augugliaro, V., L. Palmisano, and M. Schiavello. 1991. "Photon Absorption by Aqueous TiO2 Dispersion Contained in a Stirred Photoreactor." *AIChE Journal* 37: 1096–100.

Bayarri, B., J. Giménez, D. Curcó, and S. Esplugas. 2012. "Direct Evaluation of the Absorbed Photon Flow in a Photocatalytic Reactor by an Actinometric Method." *Chemical Engineering Journal* 200–202: 158–67.

Bayarri, B., J. Giménez, D. Curcó, and S. Esplugas. 2005. "Photocatalytic Degradation of 2,4-dichlorophenol by TiO2/UV: Kinetics, Actinometries and Models." *Catalysis Today* 101: 227–36.

Brucato, A., A. E. Cassano, F. Grisafi, G. Montante, L. Rizzuti, and G. Vella. 2006. "Estimating Radiant Fields in Flat Heterogeneous Photoreactors by the Six-Flux Model." *AIChE Journal* 52: 3882–90.

Bayarri, B., M. N. Abellán, J. Giménez, and S. Esplugas. 2007. "Study of the Wavelength Effect in the Photolysis and Heterogeneous Photocatalysis." *Catalysis Today* 129: 231–239.

Cabrera, M. I., O. M. Alfano, and A. E. Cassano. 1996. "Absorption and Scattering Coefficients of Titanium Dioxide Participate Suspensions in Water." *Journal of Physical Chemistry* 100: 20043–50.

Curcó, D., S. Malato, J. Blanco, J. Giménez, and P. Marco. 1996. "Photocatalytic Degradation of Phenol: Comparison between Pilot-Plant-Scale and Laboratory Results." *Solar Energy* 56: 387–400.

De La Cruz, N., V. Romero, R. F. Dantas, P. Marco, B. Bayarri, J. Giménez, and S. Esplugas. 2013. "O-nitrobenzaldehyde Actinometry in the Presence of Suspended TiO_2 for Photocatalytic Reactors." *Catalysis Today* 209: 209–14.

Galbavy, E. S., K. Ram, and C. Anastasio. 2010. "2-Nitrobenzaldehyde as a Chemical Actinometer for Solution and Ice Photochemistry." *Journal of Photochemistry and Photobiology A: Chemistry* 209: 186–92.

Giménez, J., D. Curcó, and P. Marco. 1997. "Reactor Modelling in the Photocatalytic Oxidation of Wastewater." *Water Science and Technology* 35: 207–13.

Guo, Q., C. Zhou, Z. Ma, and X. Yang. 2019. "Fundamentals of TiO2 Photocatalysis: Concepts, Mechanisms, and Challenges." *Advanced Materials*, https://doi.org/10.1002/adma.201901997.

Herrmann, J. M. 2005. "Heterogeneous Photocatalysis: State of the Art and Present Applications." *Topics in Catalysis* 34: 49–65.

Li Puma, G. and A. Brucato. 2007. "Dimensionless Analysis of Slurry Photocatalytic Reactors Using Two-Flux and Six-Flux Radiation Absorption-Scattering Models." *Catalysis Today* 122: 78–90.

Li Puma, G., J. N. Khor, and A. Brucato. 2004. "Modeling of an Annular Photocatalytic Reactor for Water Purification: Oxidation of Pesticides." *Environmental Science and Technology* 38: 3737–45.

M. Grasselli, D. P. 2008. Numerical Mathematics. Burlington: Jones & Bartlett Learning.

Malato, S., P. Fernández-Ibáñez, M. I. Maldonado, J. Blanco, and W. Gernjak. 2009. "Decontamination and Disinfection of Water by Solar Photocatalysis: Recent Overview and Trends." *Catalysis Today* 147: 1–59.

Marugán, J., R. van Grieken, C. Pablos, M. L. Satuf, A. E. Cassano, and O. M. Alfano. 2011. "Rigorous Kinetic Modelling with Explicit Radiation Absorption Effects of the Photocatalytic Inactivation of Bacteria in Water Using Suspended Titanium Dioxide." *Applied Catalysis B: Environmental* 102: 404–16.

Moreira, J., B. Serrano, A. Ortiz, and H. De Lasa. 2010. "Evaluation of Photon Absorption in an Aqueous TiO2 Slurry Reactor Using Monte Carlo Simulations and Macroscopic Balance." *Industrial & Engineering Chemistry Research* 49: 10524–34.

Moreno-SanSegundo, J., C. Casado, and J. Marugán. 2020. "Enhanced Numerical Simulation of Photocatalytic Reactors with an Improved Solver for the Radiative Transfer Equation." *Journal of Chemical Engineering* 388, https://doi.org/10.1016/j.cej.2020.124183.

Peralta Muniz Moreira, R. and G. Li Puma. 2021. "Multiphysics Computational Fluid-Dynamics (CFD) Modeling of Annular Photocatalytic Reactors by the Discrete Ordinates Method (DOM) and the Six-Flux Model (SFM) and Evaluation of the Contaminant Intrinsic Kinetics Constants [WWW Document]." *Catalysis Today*, https://doi.org/10.1016/j.cattod.2020.01.012.

Ramírez-Cabrera, M. A., P. J. Valadés-Pelayo, C. A. Arancibia-Bulnes, and E. Ramos. 2017. "Validity of the Six-Flux Model for Photoreactors." *Journal of Chemical Engineering* 330: 272–80.

Rizzo, L., A. Della Sala, A. Fiorentino, and G. Li Puma. 2014. "Disinfection of Urban Wastewater by Solar Driven and UV Lamp - TiO2 Photocatalysis: Effect on a Multi Drug Resistant Escherichia coli Strain." *Water Research* 53: 145–52.

Roda, G. C. and F. Santarelli. 2007. "A Rational Approach to the Design of Photocatalytic Reactors." *Industrial & Engineering Chemistry Research* 46: 7637–44.

Rodríguez, M., S. Malato, C. Pulgarin, S. Contreras, D. Curcó, J. Giménez, and S. Esplugas. 2005. "Optimizing the Solar Photo-Fenton Process in the Treatment of Contaminated Water. Determination of Intrinsic Kinetic Constants for Scale-Up." *Solar Energy* 79: 360–8.

Sánchez Mirón, A., E. Molina Grima, J. M. Fernández Sevilla, Y. Chisti, and F. García Camacho. 2000. "Assessment of the Photosynthetically Active Incident Radiation in Outdoor Photobioreactors Using Oxalic Acid/uranyl Sulfate Chemical Actinometer." *Journal of Applied Phycology* 12: 385–94.

Satuf, M. L., M. J. Pierrestegui, L. Rossini, R. J. Brandi, and O. M. Alfano. 2011. "Kinetic Modeling of Azo Dyes Photocatalytic Degradation in Aqueous TiO 2 Suspensions. Toxicity and Biodegradability Evaluation." *Catalysis Today* 161: 121–6.

Serpone, N. and A. Salinaro. 1999. "Terminology, Relative Photonic Efficiencies and Quantum Yields in Heterogeneous Photocatalysis. Part I: Suggested Protocol (Technical Report)." *Pure and Applied Chemistry* 71: 303–20.

Serpone, N., I. Texier, A. V. Emeline, P. Pichat, H. Hidaka, and J. Zhao. 2000. "Post-irradiation Effect and Reductive Dechlorination of Chlorophenols at Oxygen-free TiO2/water Interfaces in the Presence of Prominent Hole Scavengers." *Journal of Photochemistry and Photobiology A: Chemistry* 136: 145–55.

Tolosana-Moranchel, A., J. A. Casas, J. Carbajo, M. Faraldos, and A. Bahamonde. 2017. "Influence of TiO2 Optical Parameters in a Slurry Photocatalytic Reactor: Kinetic Modelling." *Applied Catalysis B: Environmental* 200: 164–73.

Tolosana-Moranchel, Á., A. Manassero, M. L. Satuf, O. M. Alfano, J. A. Casas, and A. Bahamonde. 2019. "TiO2-rGO Photocatalytic Degradation of an Emerging Pollutant: Kinetic Modelling and Determination of Intrinsic Kinetic Parameters." *Journal of Environmental and Chemical Engineering* 7, https://doi.org/10.1016/j.jece.2019.103406.

Volman, D. H. and J. R. Seed. 1964. "The Photochemistry of Uranyl Oxalate." *Journal of the American Chemical Society* 86: 5095–8.

Wang, C. yi, J. Rabani, D. W. Bahnemann, and J. K. Dohrmann. 2002. "Photonic Efficiency and Quantum Yield of Formaldehyde Formation from Methanol in the Presence of Various TiO2 Photocatalysts." *Journal of Photochemistry and Photobiology A: Chemistry* 148: 169–76.

Wetchakun, K., N. Wetchakun, and S. Sakulsermsuk. 2019. "An Overview of Solar/visible Light-Driven Heterogeneous Photocatalysis for Water Purification: TiO2- and ZnO-Based Photocatalysts Used in Suspension Photoreactors." *Journal of Industrial and Engineering Chemistry*, https://doi.org/10.1016/j.jiec.2018.11.025.

Supplementary Material: The online version of this article offers supplementary material (https://doi.org/10.1515/ijcre-2021-0045).